Materials Science-Poland, 40(4), 2022, pp. 105-113
http://www.materialsscience.pwr.wroc.pl/
DOI: 10.2478/msp-2022-0050

Phosphor conversion for WLEDs: YBO_3: Ce^{3+}, Tb^{3+} and its effects on the luminous intensity and chromatic properties of dual-layer WLED model

Le Thi Thuy My[1], Nguyen Le Thai[2], Thuc Minh Bui[3], Hsiao-Yi Lee[4], Nguyen Doan Quoc Anh[5,*]

[1]Faculty of Basic Sciences, Vinh Long University of Technology Education, Vinh Long Province, Vietnam
[2]Faculty of Engineering and Technology, Nguyen Tat Thanh University, Ho Chi Minh City, Vietnam
[3]Faculty of Electrical and Electronics Engineering, Nha Trang University, Nha Trang City, Vietnam
[4]Department of Electrical Engineering, National Kaohsiung University of Science and Technology, Kaohsiung, Taiwan
[5]Faculty of Electrical and Electronics Engineering, Ton Duc Thang University, Ho Chi Minh City, Vietnam

Yttrium borate phosphor co-doping Ce^{3+}, Tb^{3+} ions (YBO_3: Ce^{3+}, Tb^{3+}) is fabricated using solid state reaction, and then its luminescence is investigated through the computational energy transfer process. Under excited near-UV light, this YBO_3: Ce^{3+}, Tb^{3+} phosphor exhibits strong absorption with broad and sharp emission bands due to the 4f – 5d and 5d – 4f transitions of Ce^{3+} ions and the 4f – 4f transition of Tb^{3+} ions, respectively. The phosphor's emission chromaticity could be tunable by adjusting the concentration of doping ions. With 15% Tb^{3+} and 3% Ce^{3+} in the composition, the phosphor can gain maximum 76.7% external quantum efficacy. The phosphor is proposed for utilization in the phosphor package of white light-emitting diodes (WLEDs) to enhance their lighting performances. The findings point out that by modifying YBO_3: Ce^{3+}, Tb^{3+} concentration (5% – 10%), improvements in luminous intensities, color consistency, and color rendering indices can be observed. The higher concentration (10%) of YBO_3: Ce^{3+}, Tb^{3+} is more advantageous to the luminous flux and chromatic uniformity in cases of 4000 K and 5000 K WLEDs, while lower (5%) concentration greatly benefits those properties in the case of 3000 K WLED. Regardless of CCTs, the WLEDs show a reduction in chromatic reproduction efficiency with the increasing concentration of YBO_3: Ce^{3+}, Tb^{3+}. Hence, this green phosphor could be a good material for high-luminescence WLED, yet the modification of phosphor concentration is advisable if the simultaneous good chromaticity is desired.

Keywords: *WLEDs; YBO_3:Ce^{3+},Tb^{3+}; luminous intensity; chromatic properties; remote phosphor structure; dual-layer phosphor*

1. Introduction

The use of phosphor to convert the light from emitted photons for white light-emitting diodes has been considered as a simpler fabricating technique as it probably reduces the electronic complexity, compared to the WLED combing three red-, blue-, and green-emitting LEDs [1, 2]. Thus, the urge in finding suitable phosphor materials to combine or replace the commercially used YAG:Ce^{3+} phosphor has been immersed. The yellow phosphor YAG:Ce^{3+} though can present good luminous flux yet the shortage of red spectral energy is problematic for WLEDs require high accuracy in color reproduction [3–5]. The phosphor materials that could be most suitable for high conversion efficiency in the blue wavelength of the blue-emitting LED chip should possess good excitability and absorption strength. Research articles reported the ability of sulfide phosphors (ZnS:Cu^{+},Al^{3+} or $SrGa_2S_4$:Eu^{2+}) for the conversion efficiency from near UV wavelength to green wavelength, yet the problem is their unsuitable chemical stability for practical applications [6–9].

Yttrium borate (YBO_3) phosphors are recognized for their flexible framework arrangement that greatly influences the luminescence characteristics, while YBO_3 with rare-earth dopants, i.e. YBO_3:Tb^{3+}, is extensively studied due to its strong intensity of photoluminescence, high transparency

* E-mail: nguyendoanquocanh@tdtu.edu.vn

© Phan Xuan Le and Huu Phuc Dang 2022. This is an open access article distributed under the Creative Commons Attribution-NonCommercial-NoDerivatives 4.0 License. (http://creativecommons.org/licenses/by-nc-nd/4.0/)

in the wavelength bands of from near UV to visible ones, and good thermal and chemical stability [10, 11]. However, the rare-earth dopants with 4f – 4f narrow line emitter (i.e. Tb^{3+} and Eu^{3+}) seem to be inappropriate as their excitation band is not broad enough to match the wavelength of the pumping LED (near UV and blue spectrum regions). The solution is co-doping these 4f – 4f emitters with a suitable and efficient sensitizer to extend their excitation spectral region. Cerium ion (Ce^{3+}) is reported to be a good sensitizer for the luminescence of Tb^{3+} rare earth dopant [12, 13]. Besides, the emission peak of Tb^{3+} is compatible with the green light that is required to generate white light with intense luminous flux and moderate color rendering level. Therefore, co-doping the ions Ce^{3+} and Tb^{3+} into the YBO_3 host could take advantage of the broad emission of Ce^{3+} and essential green emission peak of Tb^{3+} to achieve the desirable luminescence intensity and color creation of WLEDs. For this reason, in this study, we use YBO_3: Ce^{3+}, Tb^{3+} for WLED models to provide a broad and sharp green emission for the improvement in white light luminous efficiency and color quality. Besides, mentioned reports barely analyzed and discussed the influences of YBO_3: Ce^{3+}, Tb^{3+} phosphor on the luminosity and color rendition of a dual-layer remote phosphor configuration. Thus, our study uses the WLEDs constructed with two-layer remote phosphor geometry in the analysis of YBO_3: Ce^{3+}, Tb^{3+} phosphor influences on the white light performances of WLEDs.

The green-emitting phosphor YBO_3: Ce^{3+}, Tb^{3+} photoluminescence properties are investigated utilizing the computations of energy transfer between the two ions Ce^{3+} and Tb^{3+} [14]. The results demonstrate that the phosphor shows nonradiative $Ce^{3+} \rightarrow Tb^{3+}$ energy transfer. The broad excitation spectrum following the strong absorption band that overlaps the wavelength of near-UV excitation source is observed with concentrations of Ce^{3+} and Tb^{3+} of 3% and 15%, respectively. Then, the optical influences of YBO_3: Ce^{3+}, Tb^{3+} phosphor on the WLED's lumen output and chromaticity are monitored with the adjustment of the green phosphor concentration. The findings reveal the potential of YBO_3: Ce^{3+}, Tb^{3+} phosphor in acquiring greater-efficiency WLED packages.

2. Experimental and computational approaches

2.1. Experimental approach

The measurements of excitation light intensity and the photoluminescence spectral intensity of the phosphor are carried out with the utilization of the Spectralon reflectance standard (SRS-99) and the heating attachment of JASCO, HPC-503. Additionally, to analyze the photoluminescence of the applied green phosphor Ce^{3+}-doped YBO_3:Tb^{3+}, the computational model of energy transfer process among Ce^{3+} and Tb^{3+} ions should be demonstrated.

2.2. Computational model

The external quantum efficacy of the green phosphor can be expressed as [15, 16]:

$$EQE = \frac{I_{em}}{I_{ex} - I_{ref}} \tag{1}$$

where EQE is the external quantum efficacy, I_{em} and I_{ex} indicate the intensities of the light emission and the excitation light of the phosphor sample, respectively, while I_{ref} exhibits the reflected excitation light that is unabsorbed by the phosphor.

The energy transfer efficiency (ETE) of $Ce^{3+} \rightarrow Tb^{3+}$ can be measured by [17–19]:

$$\eta_{et} = 1 - \frac{\eta}{\eta_o} \tag{2}$$

where η_o is the quantum yield of the ion Ce^{3+} (donor) and η is that of the ion Tb^{3+} (acceptor), while the energy transfer efficiency is indicated by η_{et}. The η_{et} is computed with the increase in Tb^{3+} concentration in the phosphor composition. The concentration of Tb^{3+} increases, the higher the probability of the $Ce^{3+} \rightarrow Tb^{3+}$ energy transfer owing to the observed increasing η_{et}. Thus, the concentration of Tb^{3+} shows significant role in modifying the ETE of this green-emitting borate phosphor. When the concentration of doped Ce^{3+} is about 3%, η_{et} is estimated at 3.2%.

The energy transfer from Ce^{3+} to Tb^{3+} is also influenced by the distances of interaction mechanism of dipole-dipole and dipole-quatrupole. Those critical distances can be expressed as follows.

$$R_{dd}{}^6 = \frac{3h^{-4}c^4Q_a}{4\pi n^4}\int \frac{f_d(E)F_a(E)}{E^4}dE \quad (3)$$

$$R_{dq}{}^8 = \frac{3h^{-4}c^4f_q\lambda_s^2Q_a}{4\pi n^4 f_d}\int \frac{f_d(E)F_a(E)}{E^4}dE \quad (4)$$

where R_{dd} is the critical distance of dipole-dipole interaction and R_{dq} is that of the dipole-quatrupole interaction. Q_a exhibits the cross-section of the Tb^{3+} absorption activity, n indicates the borate host's index of refraction, and λ_s is the energy transfer wavelength. Besides, in the transitions of diploe and quatrupole, the electronic oscillator strengths for Tb^{3+} is presented by f_d and f_q, respectively, while $f_d(E)$ expresses the donor normalized emission spectrum of Ce^{3+} and $f_a(E)$ expresses the acceptor normalized emission spectrum [20–22].

The distance between the nearest neighbor pairs of cerium and terbium (R) can be determined using the following expression [23, 24]:

$$R \approx 2\left(\frac{3V}{4\pi CN}\right)^{1/3} \quad (5)$$

where V indicates the unit cell volume, C is the sum of Ce^{3+} and Tb^{3+} concentrations, and N is the number of available ion sites. When applying the calculated critical concentrations (3% Ce^{3+} and 3.2% Tb^{3+}) to this equation, the estimated R is about 11.9 Å with N = 2, V = 108.7 Å^3 and C = 6.2% (0.062). This statistic indicates that the distance between the nearest neighbor pair is bigger than the distances of the mentioned interactions, which could be ascribed to the significant excited energy migration within the Ce^{3+} site related to the high concentration of the ion Ce^{3+}.

The attained green phosphor YBO_3:Ce^{3+},Tb^{3+} presents strong absorption under near-UV excitation wavelength owing to the 4f – 5d transitions of the ion Ce^{3+}. The relaxation route of Ce^{3+} excited energy could include five critical stages: (1) the energy migration within the Ce^{3+} ion site, (2) the 5d – 4f transitions resulting in strong and large emission band of Ce^{3+}, (3) the $Ce^{3+} \rightarrow Tb^{3+}$ nonradiative energy transfer, (4) Tb^{3+} ions' energy migration, and (5) the intense emission of Tb^{3+} via its 4f – 4f transition. The peak EQE of 76/6% can be achieved with 3% Ce^{3+} and 15% Tb^{3+} doping concentration.

3. Results and analysis

The concentration of yellow phosphor YAG:Ce^{3+} reduces as a function of increasing concentration of the green phosphor YBO_3:Ce^{3+},Tb^{3+} layer. The lower YAG:Ce^{3+} concentration is more noticeable in the case of higher CCTs (4000 K – 5000 K) of the WLED with dual-layer phosphor remote configuration, as shown in Figure 1. The decreasing concentration of YAG:Ce^{3+} phosphor is essential for the consistency of WLED's preset CCT values when doping higher amount of green phosphor YBO_3:Ce^{3+},Tb^{3+} in the phosphor package. Moreover, the lower yellow phosphor concentration could stimulate scattering ability of the phosphor layers and result in significant changes in the optical output.

Consequently, the change in YBO_3: Ce^{3+}, Tb^{3+} concentration influences the total emitted power of the WLED package, which is illustrated in Figure 2. The difference in the sum power of two YBO_3: Ce^{3+}, Tb^{3+} concentrations (5% and 10%) is obvious at 3000 K, while that figure in the case of 4000 K and 5000 K can barely see. Besides, at 5000 K, the increasing intensities in both blue and green regions are easy to observe. This means the luminous flux at each correlated color temperature (CCT) is distinct. Generally, the green emission of the phosphor package is improved with the addition of YBO_3: Ce^{3+}, Tb^{3+}, at all CCTs. However, 5% YBO_3: Ce^{3+}, Tb^{3+} shows a more remarkable enhancement of the spectra intensity than 10% YBO_3: Ce^{3+}, Tb^{3+}, at 3000 K. Meanwhile, the greater blue emission in the case of 5000 K indicates the enhancement in blue-light conversion and scattering efficiency, besides the green light one. That the blue scattering is enhanced, the higher color consistency can be attained since the larger proportion of the blue light escaping from the LED

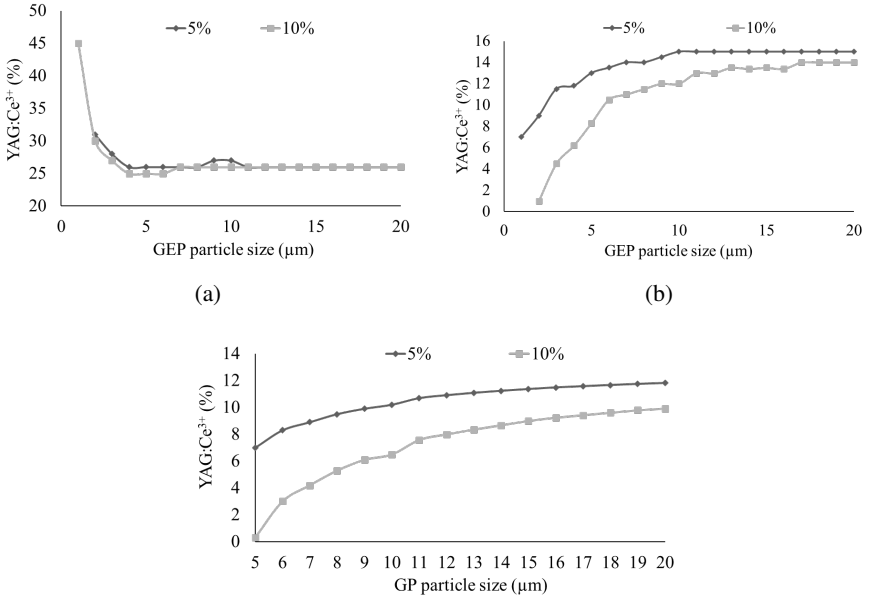

Fig. 1. The change in yellow phosphor concentration when using 5% and 10% concentrations of $YBO_3:Ce^{3+},Tb^{3+}$ at CCTs of (a) 3000 K, (b) 4000 K, (c) 5000 K

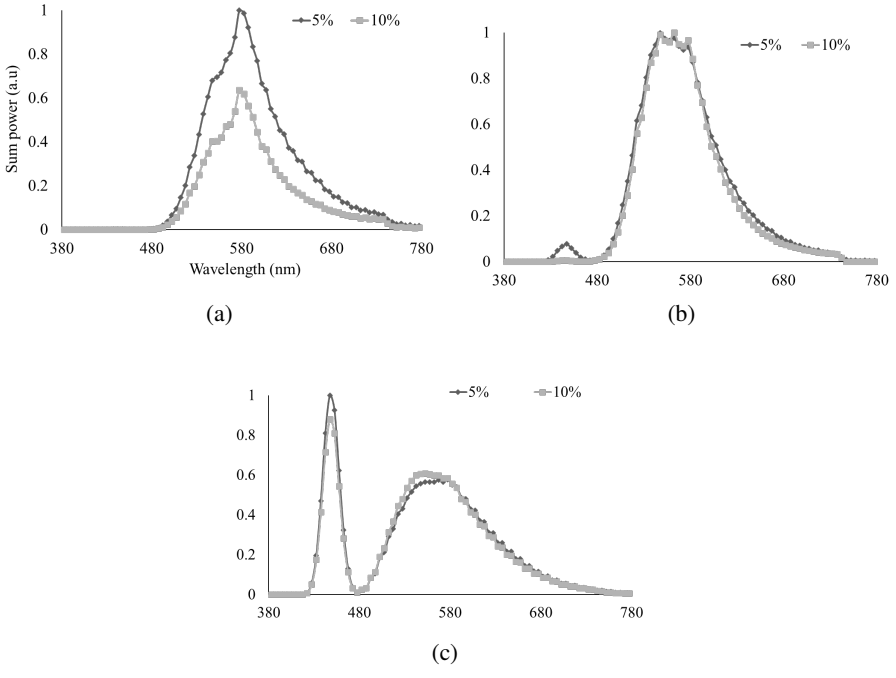

Fig. 2. WLED emission power with 5% and 10% concentrations of $YBO_3:Ce^{3+},Tb^{3+}$ at CCTs of (a) 3000 K, (b) 4000 K, (c) 5000 K

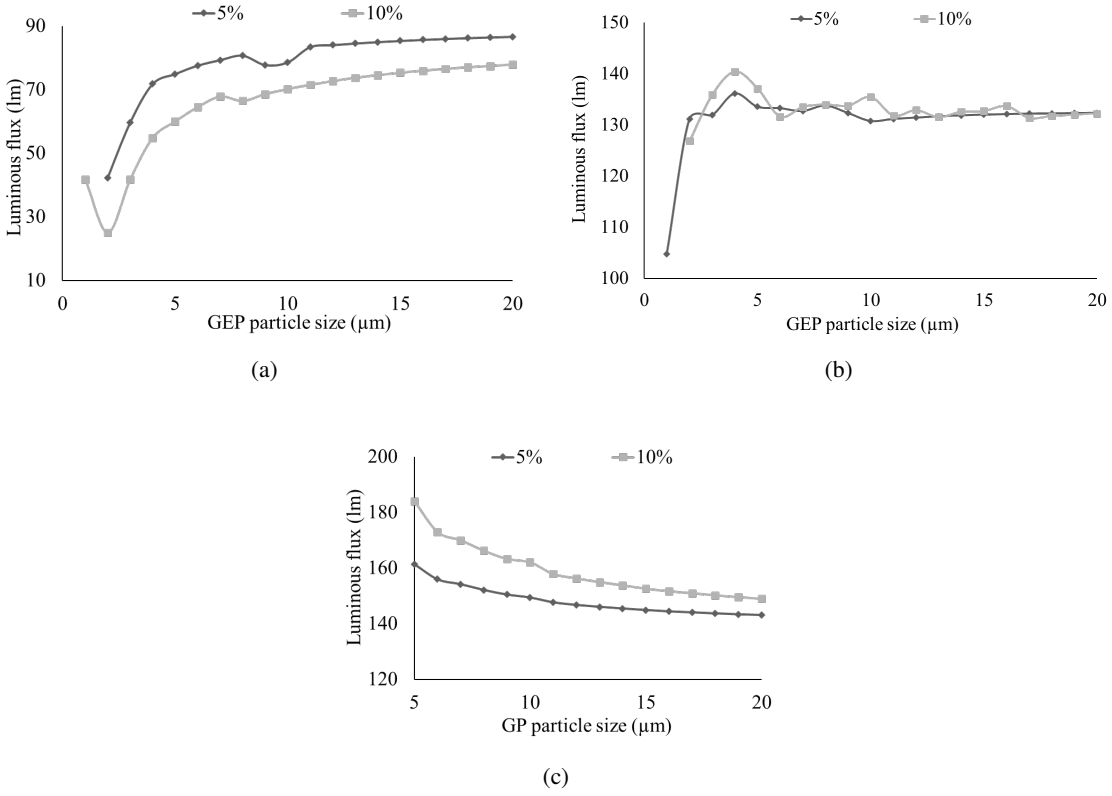

Fig. 3. Lumen output with 5% and 10% concentrations of YBO_3:Ce^{3+},Tb^{3+} at CCTs of (a) 3000 K, (b) 4000 K, (c) 5000 K

could be blended with the yellow one to form white light, or to reduce the yellow ring on the illuminated surfaces.

Regarding the total power in Figure 2(a), the luminous flux of the WLED with CCT of 3000 K could be predicted. Figure 3(a) shows that the luminous intensity of 3000-K WLED is higher with 5% concentration of YBO_3: Ce^{3+}, Tb^{3+}, with a luminescence peak at about 90 lm. At 4000 K, the difference is not really considerable between the two concentration values but the higher concentration of the green phosphor generally results in greater luminous output. Meanwhile, the luminous enhancement at higher concentration of YBO_3: Ce^{3+}, Tb^{3+} is apparently demonstrated in the case of 5000 K CCT, especially with larger particle sizes ($\geq$ 5 μm), see Figure 3(c). With 10% YBO_3: Ce^{3+}, Tb^{3+}, the highest luminous flux can be obtained at approximate 175 lm.

The consistency of chromaticity can be assessed with the color difference at a specific CCT. The lower the CCT difference, the better the color uniformity of the WLED source. Similar to the trends of the sum power and the luminous flux, the CCT variation at 3000 K with 5% YBO_3: Ce^{3+}, Tb^{3+} is lower than with 10% YBO_3: Ce^{3+}, Tb^{3+}, as shown in Figure 4(a). At 4000 K and 5000 K, the higher concentration of the green phosphor (10%) exhibits smaller variation of CCT, see Figure 4(b) and (c).

The similar changes in both luminous flux and CCT variation at three different CCTs can be attributed to the reduction of yellow phosphor and performance of sum power. Referring to Figure 1 and 2, at 3000 K, the difference in the reduction of yellow phosphor concentration is negligible between two concentrations of the green phosphor. Meanwhile, the total power is stronger with 5% of green phosphor concentration. The more in-

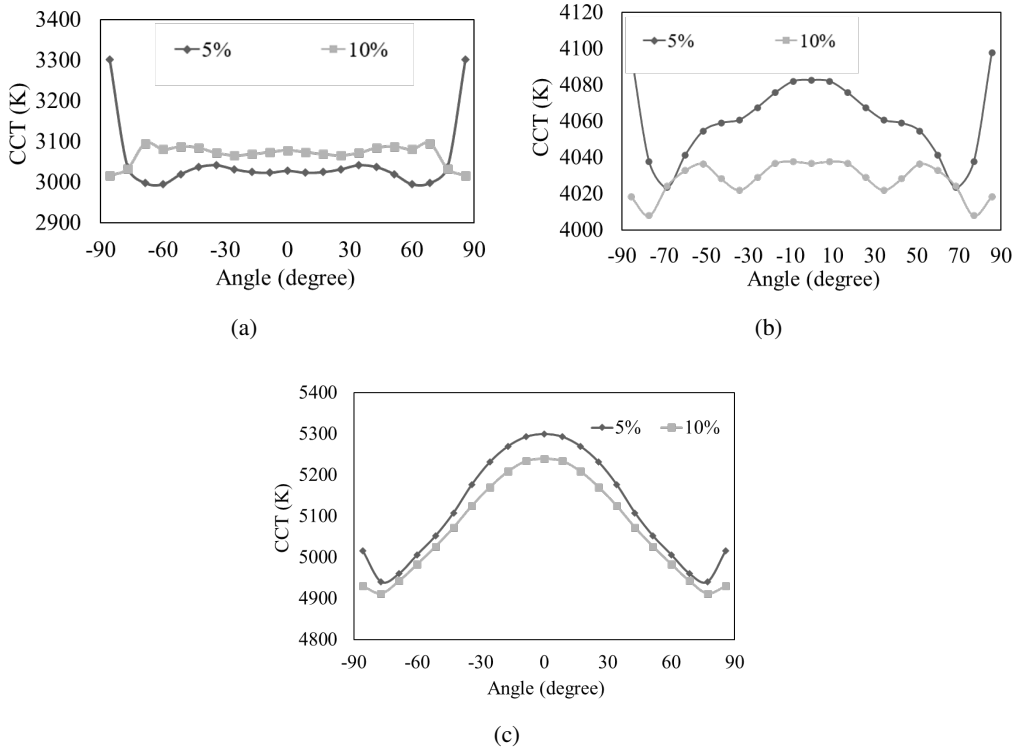

Fig. 4. CCT variances of WLEDs with 5% and 10% concentrations of YBO_3:Ce^{3+},Tb^{3+} at CCTs of (a) 3000 K, (b) 4000 K, (c) 5000 K

tense the total power, the higher the luminous output and the conversion efficiency. These enhancements probably resulted from the lower proportion of light loss and higher proportion of the light straightly extracted from the LED because of enhanced scattering. According to this, the better luminous flux and CCT consistency with 10% concentration of YBO_3: Ce^{3+}, Tb^{3+} in the cases of 4000 K and 5000 K are understandable.

The chromatic consistency is important factor in evaluating the color quality of the WLED structure. Besides, the accuracy of color reproduction is another critical factor of color assessment for white light of LEDs. The color reproduction accuracy could be performed using color rendering index CRI and color quality scale CQS. Recently, the CRI has been unfavorable for evaluating the fidelity of a light source since it is reported to give high value even in the case of bluish or reddish lights, and is not sufficient to assess the color reproduction of narrowband light sources. Thus, the CQS is introduced as an alternative to the CRI one. The CQS not only accesses the CRI aspects, but also examines the color coordinate and human factor – the comfort of eyes when interacting with the light source [25, 26]. Moreover, the color sample used for accuracy evaluation of CQS is increased to 15, not 8 samples as of the CRI. This means the chromatic reproduction is performed with smaller color gamut, leading to the higher accuracy.

Figure 5 and 6 illustrate the CRI and CQS values in relation with concentration of YBO_3: Ce^{3+}, Tb^{3+} green phosphor, respectively. The increase in green phosphor concentration is obviously disadvantageous to both CRI and CQS, regardless the CCT values. In general, the concentration of 5% results in the moderate CRI and CQS values, about 60 – 63, while that of 10% causes the CRI and CQS to decrease. This might be the downside of scattering enhancement. Particularly, the more the green phosphor scatters lights, the more the green-light components are generated. Thus, the green light is

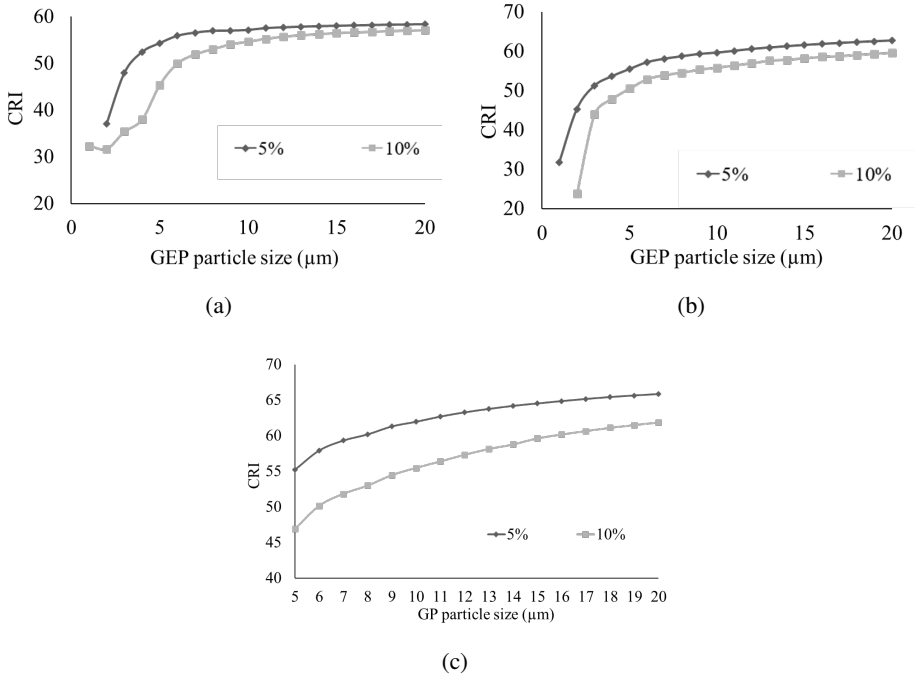

Fig. 5. CRIs of WLEDs with 5% and 10% concentrations of $YBO_3:Ce^{3+},Tb^{3+}$ at CCTs of (a) 3000 K, (b) 4000 K, (c) 5000 K

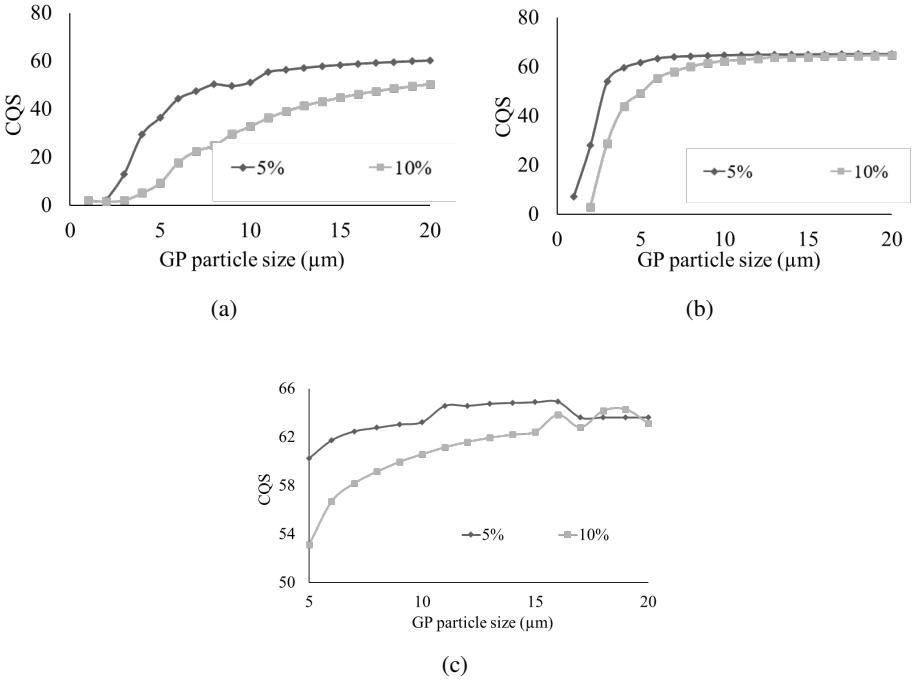

Fig. 6. CQS values of WLEDs with 5% and 10% concentrations of $YBO_3:Ce^{3+},Tb^{3+}$ at CCTs of (a) 3000 K, (b) 4000 K, (c) 5000 K

over the blue and yellow lights, which could significantly affect the accuracy of chromatic reproduction.

4. Conclusions

This work focuses on using YBO_3: Ce^{3+}, Tb^{3+} green-emitting phosphor to enhance the lighting properties of dual-layer WLED structure. Through analyzing the impacts of YBO_3: Ce^{3+}, Tb^{3+} phosphor on critical optical properties of WLEDs at three different CCTs, the phosphor is realized as a potential phosphor-conversion material for achieving the wavelength conversion efficiency in the near-UV or blue region. The great absorption strength followed by the broad emission spectrum from the 4f – 5d and 5d – 4f transitions of Ce^{3+} and the 4f – 4f transition of Tb^{3+}, respectively. The presence of the phosphor results in the enhancement of the luminescence and color consistency, owing to the improved scattering and light conversion effectiveness. The influences of CCT values and green phosphor concentration on the spectra power and color consistency are also observed. at 3000 K, 5% YBO_3: Ce^{3+}, Tb^{3+} resulted in higher values of these two factors, and vice versa at the other CCTs. The CRI and CQS, on the other hand, show decreased values with increasing concentration of YBO_3: Ce^{3+}, Tb^{3+} due to the excessive proportion of green lights, a drawback of too much scattering enhancement. The phosphor is potential to the application of high-luminescence WLED with moderate CRI and CQS of around 60 – 63, yet the recommendation is modifying the concentration of YBO_3: Ce^{3+}, Tb^{3+} green phosphor based on the determined CCT of the WLED. Though the CRI and CQS are not equal to the adequate level of 70 in this work, the optical enhancement made by YBO_3: Ce^{3+}, Tb^{3+} addition is clarified. Moreover, the photoluminescence properties of YBO_3: Ce^{3+}, Tb^{3+} are suitable with n-UV and blue-pumping LED chips. Thus, further research on YBO_3: Ce^{3+}, Tb^{3+} utilization for specific WLED devices should be carried out in the future.

References

[1] G. -F. Luo, N. T. P. Loan, L. V. Tho, N. D. Q. Anh, and H. -Y. Lee, "Enhancement of color quality and luminous flux for remote-phosphor LEDs with red-emitting $CaMgSi_2O_6$:Eu^{2+},Mn^{2+}," Materials Science-Poland **38**, 409 - 415 (2020).

[2] Z. Zhang and W. Yang, "Tunable photoluminescence in Ba1-xSrxSi3O4N2: Eu2+/ Ce3+, Li+ solid solution phosphors induced by linear structural evolution," Opt. Mater. Express **9**, 1922-1932 (2019).

[3] Y. Sun, C. Zhang, Y. Yang, H. Ma, and Y. Sun, "Improving the Color Gamut of a Liquid-crystal Display by Using a Bandpass Filter," Curr. Opt. Photon. **3**, 590-596 (2019).

[4] S. Zhao, Q. Mo, W. Cai, H. Wang, and Z. Zang, "Inorganic lead-free cesium copper chlorine nanocrystal for highly efficient and stable warm white light-emitting diodes," Photon. Res. **9**, 187-192 (2021).

[5] J. Li, D. Han, J. Zeng, J. Deng, N. Hu, and J. Yang, "Multi-channel surface plasmon resonance biosensor using prism-based wavelength interrogation," Opt. Express **28**, 14007-14017 (2020).

[6] X. Guo and N. Chi, "Superposed 32QAM Constellation Design for 2 × 2 Spatial Multiplexing MIMO VLC Systems," J. Lightwave Technol. **38**, 1702-1711 (2020).

[7] Y. Yang, C. Chen, P. Du, X. Deng, J. Luo, W. Zhong, and L. Chen, "Low complexity OFDM VLC system enabled by spatial summing modulation," Opt. Express **27**, 30788-30795 (2019).

[8] R. Fan, S. Fang, C. Liang, Z. Liang, and H. Zhong, "Controllable one-step doping synthesis for the white-light emission of cesium copper iodide perovskites," Photon. Res. **9**, 694-700 (2021).

[9] Y. Fei and J. Zhang, "Luminescence properties of KBaYSi2O7:Ce/Eu-Tb phosphors for multifunctional applications," Appl. Opt. 58, 4740-4745 (2019).

[10] A. Ahmad, A. Kumar, V. Dubey, A. Butola, B. S. Ahluwalia, and D. S. Mehta, "Characterization of color cross-talk of CCD detectors and its influence in multispectral quantitative phase imaging," Opt. Express **27**, 4572-4589 (2019).

[11] F. Jiang, J. Zhang, L. Xu, J. Ding, G. Wang, X. Wu, X. Wang, C. Mo, Z. Quan, X. Guo, C. Zheng, S. Pan, and J. Liu, "Efficient InGaN-based yellow-light-emitting diodes," Photon. Res. **7**, 144-148 (2019).

[12] Y. Li, J. Lan, W. Wang, Y. Zheng, W. Xie, X. Tang, D. Kong, Y. Xia, Z. Lan, R.Li, X. He, and G. Li, "395 nm GaN-based near-ultraviolet light-emitting diodes on Si substrates with a high wall-plug efficiency of 52.0%@350 mA," Opt. Express **27**, 7447-7457 (2019).

[13] Y. Wang, G. Xu, S. Xiong, and G. Wu, "Large-field step-structure surface measurement using a femtosecond laser," Opt. Express **28**, 22946-22961 (2020).

[14] M. Hu, J. Luo, S. Li, J. Liu, J. Li, Z. Tan, G. Niu, Z. Wang, and J. Tang, "Broadband emission of double perovskite Cs2Na0.4Ag0.6In0.995Bi0.005Cl6:Mn2+ for single-phosphor white-light-emitting diodes," Opt. Lett.

44, 4757-4760 (2019).

[15] Y. Chang, C. Liu, Z. Pei, S. Lee, Y. Lai, P. Han, H. Shih, and W. Cheng, "New scheme of LiDAR-embedded smart laser headlight for autonomous vehicles," Opt. Express **27**, A1481-A1489 (2019).

[16] B. Swiatczak, M. Feldkaemper, and F. Schaeffel, "Changes in fundus reflectivity during myopia development in chickens," Biomed. Opt. Express **10**, 1822-1840 (2019).

[17] Y. Shi, S. Ye, J. Yu, H. Liao, J. Liu, and D. Wang, "Simultaneous energy transfer from molecular-like silver nanoclusters to Sm3+/Ln3+ (Ln=Eu or Tb) in glass under UV excitation," Opt. Express **27**, 38159-38167 (2019).

[18] L. Zhang, C. Wang, Y. Jin, and T. Xu, "Wide color gamut white light-emitting diodes based on two-dimensional semiconductor nanoplatelets," Opt. Express **30**, 3719-3728 (2022).

[19] J. Lui, A. M. Vegni, L. Colace, A. Neri, and C. Menon, "Preliminary design and characterization of a low-cost and low-power visible light positioning system," Appl. Opt. **58**, 7181-7188 (2019).

[20] P. Kumar and N. K. Nishchal, "Enhanced exclusive-OR and quick response code-based image encryption through incoherent illumination," Appl. Opt. **58**, 1408-1412 (2019).

[21] S. Gong, R. Wu, S. Yang, L. Wu, M. Zhang, Q. Han, and W. Wu, "Tuning the luminous properties and optical thermometry of Cs2SnCl6 phosphor microcrystals via Bi and Sb codoping," Photon. Res. **9**, 2182-2189 (2021).

[22] B. Yu, Z. Lu, G. Liang, Y. Yuan, H. Wang, J. He, and S. Yang, "Luminous efficacy enhancement for LED lamps using highly reflective quantum dot-based photoluminescent films," Opt. Express **29**, 29007-29020 (2021).

[23] C. Huang, Y. Chang, L. Han, F. Chen, S. Li, and J. Hong, "Bandwidth correction of spectral measurement based on Levenberg–Marquardt algorithm with improved Tikhonov regularization," Appl. Opt. **58**, 2166-2173 (2019).

[24] E. L. Francois, J. Herrnsdorf, J. J. D. McKendry, L. Broadbent, G. Wright, M. D. Dawson, and M. J. Strain, "Synchronization-free top-down illumination photometric stereo imaging using light-emitting diodes and a mobile device," Opt. Express **29**, 1502-1515 (2021).

[25] Q. Liu, Y. Liu, M. R. Pointer, Z. Huang, X. Wu, Z. Chen, and M. R. Luo, "Color discrimination metric based on the neutrality of lighting and hue transposition quantification," Opt. Lett. **45**, 6062-6065 (2020).

[26] H. Q. T. Bui, R. T. Velpula, B. Jian, M. R. Philip, H. D. Tong, T. R. Lenka, and H. P. T. Nguyen, "High-performance nanowire ultraviolet light-emitting diodes with potassium hydroxide and ammonium sulfide surface passivation," Appl. Opt. **59**, 7352-7356 (2020).

Received 2022-05-13
Accepted 2022-11-28